New Diagnostic of the Most Populated Conformer of Tetrahydrofuran in the Gas Phase

Tiecheng Yang,[†] Guolin Su,[†] Chuangang Ning,[†] Jingkang Deng,*[,†] Feng Wang,*[,‡] Shufeng Zhang,[†] Xueguang Ren,[†] and Yanru Huang[†]

Department of Physics and Key Laboratory of Atomic and Molecular NanoSciences of MOE, Tsinghua University, Beijing 100084, People's Republic of China, and Centre for Molecular Simulation, Swinburne University of Technology, P. O. Box 218, Hawthorn, Melbourne, Victoria 3122, Australia

Received: September 25, 2006; In Final Form: February 12, 2007

The most populated conformer of tetrahydrofuran (C_4H_8O) has been diagnosed as the C_s conformer in the present study, jointly using experimental electron momentum spectroscopy (EMS) and quantum mechanics. Our B3LYP/6-311++G** model indicates that the C_1 conformation, which is one of the three possible conformations of tetrahydrofuran produced by pseudorotation in the gas phase, is a transition state due to its imaginary frequencies, in agreement with the prediction from a recent ab initio MP2/aug-cc-pVTZ study (*J. Chem. Phys.* **2005**, *122*, 204303). The study has identified the fingerprint of the highest occupied molecular orbital (HOMO) of the C_s (12a′) conformer as the most populated conformer. The identification of the C_s structure, therefore, leads to the orbital-based assignment of the ionization binding energy spectra of tetrahydrofuran for the first time, on the basis of the outer valence Green function OVGF/6-31G* model and the density functional theory (DFT) SAOP/ET-PVQZ model. The present study explores an innovative approach to study molecular stabilities. It also indicates that energetic properties are not always the most appropriate means to study conformer-rich biological systems.

1. Introduction

Structures of many biologically active compounds include a tetrahydrofuran (THF) fragment. Tetrahydrofuran is a prototype of heterocyclic five-member-ring structures and an important structural unit of carbohydrates and biological molecules.[1] In particular, THF can be viewed as an analogue of the sugar moiety in the sugar−phosphate backbone of deoxyribonucleic acid (DNA) and ribonucleic acid (RNA).[2] The sugar moiety occupies a central position in the structure of nucleic acids and is of crucial importance in shaping their structure and dynamics. For example, a striking difference exists in properties between DNA and RNA, which differ only by their chemical nature of the sugar. The determination of electronic structures of isolated fragments of DNA is an important step toward the understanding of mechanisms for secondary structures of DNA and its damage.[3] Derivatives of THF are widely prescribed for a variety of diseases, such as nucleoside antibiotics. For example, azidothymidine (AZT) is commonly recognized as the first anti-AIDS drug used in antiviral chemotherapy and prophylaxis in the United States.[4]

Largely existed as conformers and tautomers, biological molecules exhibit the uniqueness and complexity. In these species, compounds and fragments interact in a defined arrangement, with not only the chemical composition but also their precise stereochemistry. THF, like other molecules with five-member rings, is not planar but puckered. It displays an internal motion known as pseudorotation,[5] which was originally postulated for cyclopentane.[6] Conformations of THF are flexible along the pseudorotation path[7,8] as a function of the pseudorotation angle φ. For example, the THF conformers at $\varphi = 0°$ and 180° possess the C_s point group symmetry (E, envelope), conformers at $\varphi = \pm 90°$ have the C_2 symmetry (T, twisted), and conformations at other angles such as $\varphi = \pm(50-60°)$ and $\varphi = \pm(120-130°)$ exhibit the C_1 symmetry as indicated by the MP2/aug-cc-pVTZ model.[9]

The preferred (most stable or most populated) conformation of tetrahydrofuran is not precisely known so far. Although a number of theoretical and experimental studies[1,6−15] have tackled THF, the analyses do not provide a definitive answer[16] and the findings are either contradictory or insensitive to the pseudorotation angle. In addition, the results largely depend on the models used (theory) and methods of experimental data manipulation. For example, studies of Meyer et al.[8] and Engerholm et al.[14] indicated that the minima associated with the C_1 symmetry were the global minima for THF, whereas Melnik et al.[12] and Mamleev et al.[15] reported completely different minima and maxima structures for THF, leading to a stability ordering of $C_2 > C_s > C_1$; the stability ordering of $C_2 > C_1 > C_s$ was given by Cadioli et al.[1] on the basis of the Hartree−Fock (HF) and second-order Moller−Plesset (MP2) calculations. The C_2 structure of THF in crystal was found by Luger and Buschman.[16] Most recently, Rayón and Sordo[9] suggested another possibility of the stability order as $C_s > C_2$, on the basis of the MP2 theory and Dunning's large basis sets.

There is no single approach which is best for all purposes.[17,18] Small and subtle energy differences among the conformations of tetrahydrofuran are within the error bars of many quantum mechanical models.[19] Rayón and Sordo[9] further indicated that very different potential energy cross-sections of THF as a function of the pseudorotation motion were associated with different basis sets. The predicted minimal structures with one model, for example, the C_s symmetry of THF using the MP2/aug-cc-pVTZ model, might be a transition state with imaginary frequencies from another model, for example, the MP2/cc-pVDZ

* Corresponding author. E-mail: djk-dmp@tsinghua.edu.cn (J.D.); fwang@swin.edu.au (F.W.).
† Tsinghua University.
‡ Swinburne University of Technology.

10.1021/jp066299a CCC: $37.00
Published on Web 05/19/2007

model.[9] As a result, energetic properties are obviously not so sensitive in the determination of the stability of the conformations produced by pseudorotation. Although it would be inappropriate to assume that higher level theory always provides more accurate results,[20] the study[9] indeed indicates that the critical competition is, in fact, between the THF conformers of the C_2 and C_s structures.

When predicting future progress in quantum chemistry many years ago, Coulson[21] pointed out that "the most important clue seems to be the recognition that the energy is not the only criterion of goodness of wave functions." In this paper, instead of concentrating on conventional energetic properties, we explore an innovative approach to differentiate the C_2 and C_s conformers of THF, i.e., using dual space analysis (DSA)[17] through the identification of symmetries of the highest occupied molecular orbitals (HOMO) of the C_2 (9b) and C_s (12a′) conformers, jointly based on an electron momentum spectroscopic (EMS) measurement and theoretical calculations. The measured orbital electron momentum profile, in conjunction with theoretical simulations for the HOMOs, is able to provide information of the most populated conformer of THF in the gas phase under the experimental conditions.

2. Experimental Details

The claimed purity of the sample tetrahydrofuran purchased is 99.0%. The measurement, therefore, proceeded without further purification. No impurity of the sample was evident in the binding-energy spectra.

The EMS measurements for THF were undertaken with the symmetric non-coplanar geometry using a high-resolution and high-sensitivity (e, 2e) electron momentum spectrometer recently developed at Tsinghua University.[22] With the novel double toroidal analyzer and the two-dimension position-sensitive detectors, the collect efficiency is about 2 orders of magnitude higher than that of our previous spectrometer,[23,24] so the statistical accuracy and the reliability have been improved significantly. In a number of recent EMS experiments aiming at testing the plane wave impulse approximation (PWIA), the Tsinghua EMS experimental group has been able to achieve a wider range of impact energies, from as low as 400 eV to as high as 2400 eV[26−28] for molecules such as ethylene,[26] HOMOs of 1,3-cyclohexadiene,[27] and HOMO of oxygen.[28] It has been indicated that although a certain degree of variation in orbital momentum distributions (MDs) in small and large momentum regions is observed, the fundamental shape of orbital momentum distribution remains when the impact energy varies. The incident energies in the present experiment were 600 and 1200 eV plus binding energies, respectively. However, the spectra at the impact energy of 1200 eV is poor and further work in this direction is carrying on at the moment.

This new upgraded EMS spectrometer has significantly achieved the angular resolution of $\Delta\theta = \pm 0.7°$ and $\Delta\phi = \pm 1.9°$, with an energy resolution of $\Delta E = \pm 1.2$ eV (full width at half-maximum (fwhm)). The EMS binding energy spectra from the measurement were deconvoluted using a least-squares fit according to Bevington and Robinson[25] into Gaussians with fixed peak widths and positions but variable Gaussian heights (relative cross-sections). The procedure of extracting experimental MDs from those angular resolved energy spectra can be found in our previous work.[29] In addition, the normalization of the measured orbital momentum distributions to the simulated in the theory is one of the general normalization methods used in the EMS field, employed by the Brion group at the University of British Columbia.[50,58] The procedure is to compare the experimental MDs with theoretical ones; the observed MDs were divided by a normalized constant to give a best fit.

3. Methods and Computational Details

Dual space analysis (DSA)[17] is employed in the present work. Information obtained in position and momentum spaces is complementary, and they are connected by the uncertainty principle, which in one-electron systems may be interpreted as a statement about the correlation between measurement of the coordinates **r** and momenta **p**. The mutual information density in momentum space illustrates that this localization is accompanied by strong correlation at small values of **p**.[30] Momentum space information such as orbital momentum distributions[30−35] and momentum space maps[36] are particularly convenient for the determination of contributions to a given molecular orbital from orbitals associated with particular atoms.[30]

Electronic structural calculations for the ground state of tetrahydrofuran with a C_s symmetry (X^1A'), a C_2 symmetry (X^1A), and a C_1 symmetry (X^1A) are performed using three parallel quantum mechanical models—B3LYP, OVGF, and SAOP. Guassian type basis sets of 6-31G* and 6-311++G** are employed with respect to the OVGF and B3LYP models. Here the OVGF/6-31G* model is the outer valence electron propagator (Green's function) model,[37,38] whereas the SAOP/ET-PVQZ model is an orbital-dependent statistical average of orbital potential (SAOP) functional.[39,40] The ET-PVQZ basis set is an even-tempered Slater type basis set.[41] The B3LYP/6-311++G** model is employed to generate a number of molecular properties and orbital densities in coordinate space, whereas the OVGF/6-31G* and SAOP/ET-PVQZ models are employed to generate reliable vertical ionization potentials in the outer valence space of the THF conformers. The calculated orbital energies are employed to assist the assignment of the binding energy spectra observed from photoelectron spectroscopy (PES)[42] and the present EMS. All electronic structural calculations according to the B3LYP/6-311++G**, OVGF/6-31G*, and SAOP/ET-PVQZ models are based on the optimized geometries generated using the MP2/aug-cc-pVTZ model[9] by means of computational chemistry packages such as GAUSSIAN98, GAUSSIAN03,[43] and Amsterdam Density Functional (ADF) suite of programs.[41]

Under the Born−Oppenheimer approximation, independent particle approximation, and the plane wave impulse approximation (PWIA),[44,45] the triple differential EMS cross-section (momentum distribution, σ) is given by[44,45]

$$\sigma_{\mathrm{EMS}} \propto \int \mathrm{d}\Omega |\langle p\Psi_f^{N-1}|\Psi_i^N\rangle|^2 \qquad (1)$$

The overlap of the ion and neutral wave functions in eq 1 is known as the Dyson orbital.[46] The Dyson orbital can be directly calculated either by configuration interaction (CI)[47] or by Green function (GF)[48] methods, which are highly demanding for computation power. The Dyson orbitals can be closely further approximated with the Kohn−Sham orbitals of DFT (TKSA);[49] then eq 1 is simplified as

$$\sigma_{\mathrm{EMS}} \propto S_i^f \int \mathrm{d}\Omega |\psi_i(p)|^2 \qquad (2)$$

where $\psi_i(p)$ is the momentum space canonical Kohn−Sham orbital and S_i^f is the pole strength. The quantity $\int \mathrm{d}\Omega$ gives the spherical average over the random orientations of the gas-phase target molecules.

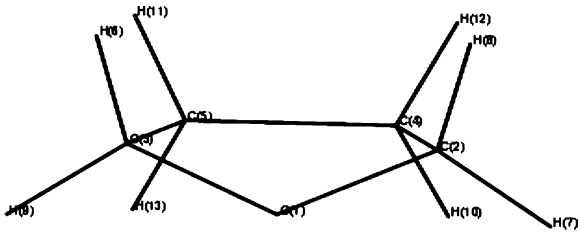

Figure 1. Molecular structure of tetrahydrofuran and the atomic numbering system.

TABLE 1: Molecular Properties of the Tetrahydrofuran Conformers Calculated Using the B3LYP/6-311++G Model**[a]

property	C_s	C_2	C_1
ground state	X^1A'	X^1A	X^1A
HOMO	12a′	9b	20a
first IP (eV)	10.32	10.01	10.24
R_5[b] (Å)	7.450	7.535	7.403
μ[c] (D)	1.83	1.89	1.91
E/E_h	−232.541 593	−232.541 463	−232.541 471
ν_i[c] (cm^{-1})	35.18	47.48	33.84i

[a] The optimized geometries of the conformers are based on MP2/aug-cc-pVTZ of ref 9. [b] Ring perimeter (R_5) is defined as a simple sum of the bond lengths of constituent bonds of the ring. See ref 56. [c] μ = dipole moment. [d] The lowest frequency (ν_i) is generated at the B3LYP/6-311++G** level using optimization in the present work.

In the present work, the KS orbitals are produced by the B3LYP/6-311++G**//MP2/aug-cc-pVTZ model in coordinate space, from which the orbital MDs of the C_2 and C_s tetrahydrofuran conformers are simulated using the HEMS program[50] via the Fourier transform given in eq 1. Experimental conditions, that is, the impact energy given by 600 eV (plus binding energies) and the effects of the finite acceptance angles of the experimental spectrometer in both θ and ϕ given by $\Delta\theta \approx \pm 0.7°$ and $\Delta\phi \approx \pm 1.9°$, are incorporated in the simulation with the Gaussian method.[51] Note that the azimuthal angle ϕ in EMS is a completely different concept from the pseudorotation angle φ of THF.

4. Results and Discussions

4.1. Molecular Properties of Tetrahydrofuran. Structure and atom numbering of the saturated THF are given in Figure 1. That is, the numbering starts from the ether oxygen, O(1); the carbon atoms directly connected to O(1) are C(2) and C(3), whereas the other carbon atoms which do not directly connect to O(1) are C(4) and C(5). The energy differences among the three conformations of THF are so small so that they are right within the error bars of many computational chemistry models[9,31] from the levels of theory and basis sets. For example, it is noted that, on the basis of the B3LYP/6-311++G**//MP2/aug-cc-pVTZ model, the conformation with the C_s symmetry gives the lowest energy of the three conformations, followed by the C_1 conformer, and the C_2 conformer yields the highest energy. However, the present B3LYP/6-311++G** optimizations give the order of stability as $C_2 > C_1 > C_s$. The stability of the C_s conformer predicted by two models is completely opposite. More definite information rather than energetic properties is, therefore, required as the indicator of the conformer stability.

Table 1 compares a number of more anisotropic properties of the three conformations (C_1, C_s, and C_2) of tetrahydrofuran. Anisotropic properties such as dipole moments have been very sensitive properties to the changes of electron charge distributions for rotational conformers of a number of biological species.[30,31,52] The conformer properties given in Table 1 indicate that this is not the case for THF conformers produced by pseudorotation. Only subtle differences are exhibited in these properties, including dipole moment, as the species undergoes pseudorotation. For example, the dipole moments for C_1, C_s, and C_2 conformations are given by 1.91, 1.83, and 1.89 D, respectively. Although the MP2/aug-cc-pVTZ model[9] and the B3LYP/6-311++G** model both predict different stability ordering of the THF conformations, what is common with these models is that both of them produce a negative lowest frequency for the C_1 structure, leading to the transition-state status for the C_1 conformation. As a result, the issue now is to identify the relative stability between conformers of the C_s and C_2 symmetries.

Many molecular properties of the C_s and C_2 structures do not vary substantially. There is, however, a significant difference in their molecular electron charge (derived) potential (MEP). Figure 2 displays the MEP of the C_2 (Figure 2a) and the C_s (Figure 2b) structures, in which the projection is based on a plane formed by the C(2)−O(1)−C(3) network for both cases. Certain electron distribution patterns with respect to their own molecular structure are indeed demonstrated in the MEPs. For example, in the C_2 case, the MEP is dominated by positive charges, whereas, in the C_s case, the electron charge distributions in the C(2)−O(1)−C(3) network concentrate on the hydrogen atoms for positive signs but negative signs for the oxygen and carbon atoms are observed. There is indeed little that is analogous in the MEPs of the two conformers, indicating that the conformers may be associated with very different electron density distributions.

4.2. Binding Energy (Ionization) Spectra for Tetrahydrofuran. In the present EMS experiment, the binding energy spectra of THF obtained at the azimuthal angle ϕ over the range of 0 to ±30° (a) and at $\phi = 0°$ (b) are shown in Figure 3 (impact electron energy of 600 eV plus binding energies). In the outer valence space (<20 eV), five peaks have been determined at 9.7, 11.9, 14.1, 16.3, and 19.3 eV, respectively, as shown by the vertical bars in Figure 3b. The present EMS measured binding energies are given in Table 2, together with the results of the high-resolution PES[42] of tetrahydrofuran. Although good agreement in spectral line position between the two experiments has been achieved, like many other organic and/or biomolecular species, the observed spectra are largely congested as seen in Figure 3. It is noted that both PES and EMS measurements themselves do not provide definite information on orbital-based ionization spectral assignment, so that the spectral assignment can only rely on very accurate theoretical calculations, upon the identification of the most stable structure under the experimental conditions. It is noted that a very broad Gaussian with a peak position of ca. 25 eV is seen in the binding energy spectra in Figure 3. The broad peak does not correlate to any orbitals in the valence shell. This unrealistic Gaussian may be caused by the fitting procedure employed in the present study, since the fitting was performed to achieve the best fit, rather than the most physically reasonable fit (the latter approach avoids such unphysical gaussians but may reduce the independence of measurements).

A combination of two accurate models, that is, the outer valence Green function (OVGF/6-31G*) model and the density functional theory based SAOP/ET-PVQZ model, is employed to produce the orbital-based ionization energies of the species. The OVGF model accurately predicts the positions of spectral peaks in the binding energy spectra, but the model itself relies on the orbital irreducible representatives given by the corre-

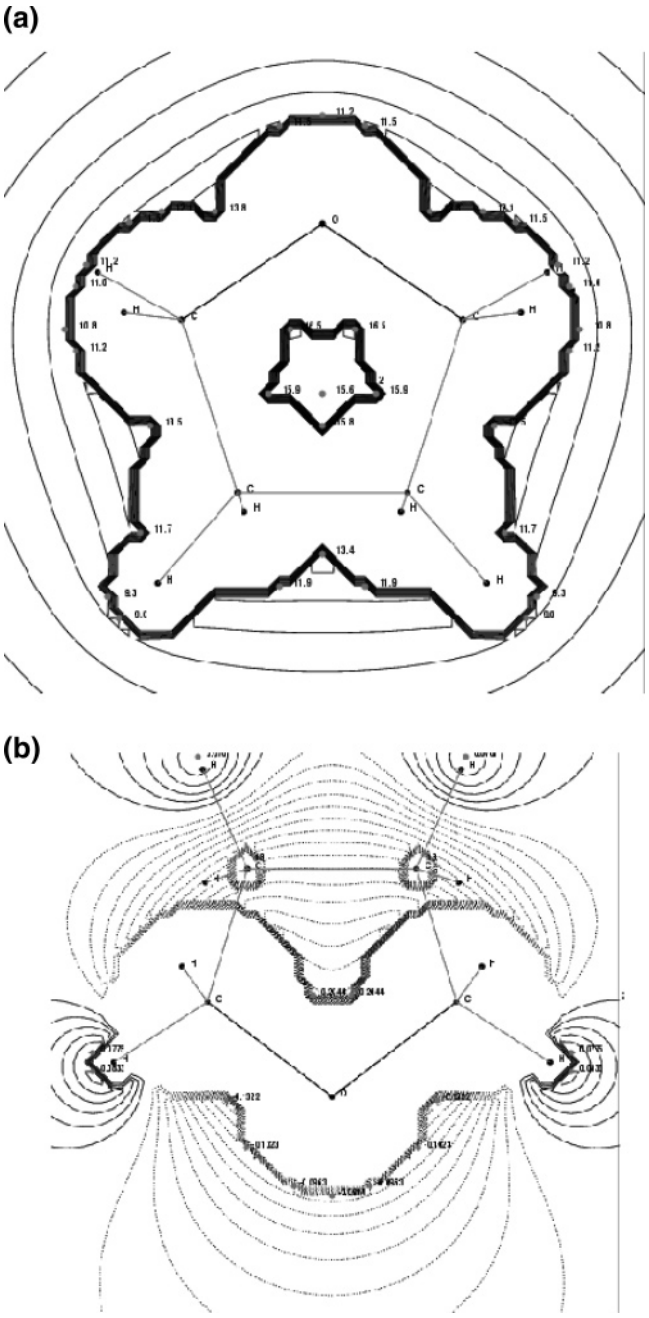

Figure 2. Molecular electron charge (derived) potentials (MEPs) for tetrahydrofuran of (a) the C_2 conformer and (b) the C_s conformer.

sponding HF method. If, due to electron correlation, the electronic configuration of a species is not the same as the one obtained from the HF method (which is the case in most situations), the results from the OVGF model are only useful for ionization energies rather than for orbital assignment. For this reason, the SAOP/ET-PVQZ model is employed in the present study, as the SAOP/ET-PVQZ model produces good ionization energy spectra for molecules using the meta-Koopman's theorem[53] as well as the associated orbital irreducible representations (note that the matrices in the SAOP model are diagonalized on the basis of their individual irreducible representatives). Table 2 reports the binding energy spectra of the C_2 and C_s conformers of THF calculated using OVGF/6-31G* and SAOP/ET-PVQZ models, together with the observed PES and EMS experimental spectral peak positions. However, orbital-based assignment to the binding energy spectra could only be

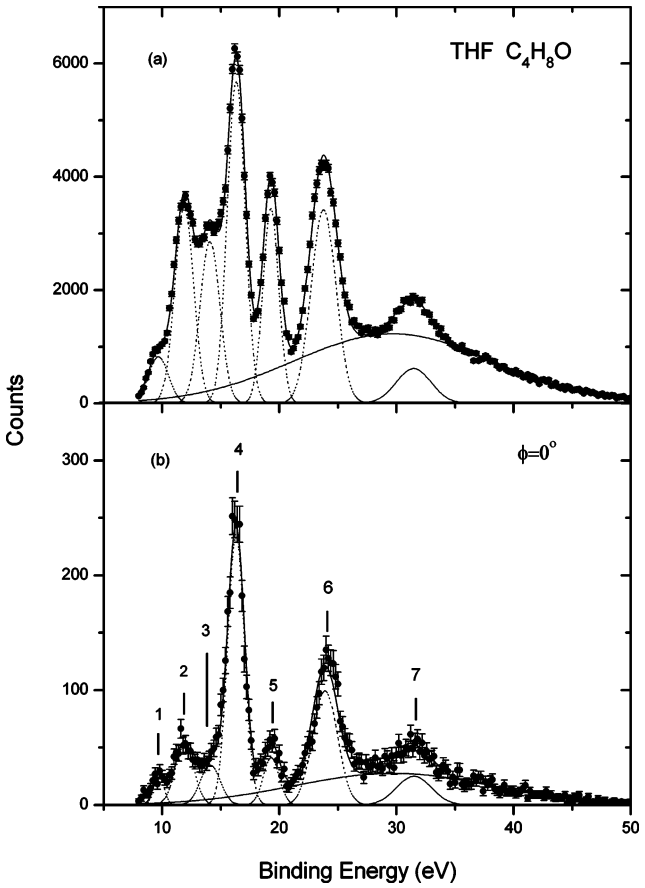

Figure 3. Electron momentum spectroscopic binding energy spectra of tetrahydrofuran at the azimuthal angle ϕ (a) over the range of 0° to ±30° and (b) $\phi = 0°$. The dashed lines represent Gaussian fits to the peaks, and the solid curves are the summed fits. The determined peaks are marked as vertical bars in b.

determined, once the most stable structure in the gas phase, C_2 or C_s, is identified.

4.3. Diagnostic of the C_s Conformer of Tetrahydrofuran in the Gas Phase. Diagnostic of the most populated conformer of tetrahydrofuran in the gas phase provides a showcase for the mutual dependence of experiment and theory. Without any of them, the results would exhibit a large degree of uncertainties. In the present study, theoretical calculations have excluded the C_1 conformation as a transition state with imaginary frequencies from the group of three possibilities (C_1, C_2, and C_s). For the remaining two conformers of THF (C_2 and C_s), our calculations (OVGF/6-31G* and SAOP/ET-PVQZ) have produced accurately the binding energies in the outer valence space, in agreement with the PES and the present EMS measurements. However, even though the present calculations and some previous studies[9] indeed suggested that the C_s structure is in favor with a subtly lower energy, comparing to the C_2 structure, such a small energy difference does not give us sufficient confidence without solid experimental evidence. The orbital irreducible representatives of the HOMO for the C_s and C_2 conformers, fortunately, are very different since the conformers belong to different point group symmetries. For the C_s conformer, the HOMO is 12a′, whereas the HOMO is 9b for the C_2 conformer of THF.

The HOMOs of the C_2 (b) and C_s (a′) conformers will split according to their symmetries in momentum space when presented in orbital momentum distributions. To identify the conformation of THF, it is important to resolve and to detremine the binding energy spectral line (peak 1 in Figure 3) for the

TABLE 2: Assignment of the Experimental Binding Energy Spectra of Tetrahydrofuran in the Outer Valence Shell Using OVGF/6-31G* and SAOP/ET-PVQZ Calculations (eV)

theory						
C_2		C_s			experiment	
OVGF 6-31G*(SP)[a]	SAOP ET-PVQZ	OVGF 6-31G*(SP)[a]	SAOP ET-PVQZ	C_s assignmt	PES[b]	EMS
9.38 (0.92)	10.01 (9b)	9.63 (0.92)	10.32 (12a′)	**12a′**	9.74	9.7
11.11 (0.91)	11.67 (11a)	11.36 (0.91)	11.93 (11a′)	**11a′**	11.52	11.9
11.85 (0.93)	12.11 (10a)	11.65 (0.93)	11.97 (8a″)	**8a′**		
12.08 (0.92)	12.51 (8b)	11.86 (0.92)	12.40 (7a″)	**7a″**		
12.30 (0.92)	12.75 (9a)	12.11 (0.91)	12.72 (10a′)	**10a′**	12.52	
14.06 (0.92)	13.98 (7b)	13.69 (0.92)	13.84 (6a″)	**6a″**	14.1	14.1
14.72 (0.92)	14.48 (8a)	14.28 (0.91)	14.23 (9a′)	**11a′**	14.5	
14.72 (0.91)	14.76 (6b)	15.13 (0.91)	15.12 (5a″)	**5a″**	15.4	
16.54 (0.91)	16.22 (7a)	16.15 (0.90)	15.99 (8a′)	**8a′**	16.8	16.3
16.91 (0.91)	16.51(5b)	16.66 (0.91)	16.31 (7a′)	**7a′**		
	18.64(6a)		18.67 (4a″)	**4a″**	19.5	19.3
	18.88 (4b)		18.91 (6a′)	**6a′**		

[a] Here SP is the spectroscopic pole strength factor calculated by the OVGF model. [b] The He I photoelectron spectrum of tetrahydrofuran from ref 42 without being assigned to particular orbitals.

HOMO of the species. Fortunately, the energy separations of peak 1 (the HOMO) and peak 2 for both the C_2 or C_s conformers of THF are sufficiently large (>1.50 eV, refer to Table 2), so that the EMS technique with an instrumental energy resolution of ±1.2 eV (fwhm) is able to resolve peak 1. Although there exists a certain overlap between peaks 1 and 2 in Figure 3a—in fact, peak 1 is presented as a "hump" in this figure—the position of peak 1 (HOMO) at 9.4 eV is clearly resolved in the binding spectrum at $\phi = 0°$ in Figure 3b of the present EMS measurement. The first peak at 9.7 eV is evidenced by the previous PES measurement[42] with a much higher resolution and is supported by our quantum mechanical calculations given in Table 2. It is noted that the likely "peak" in the leading edge of the first Gaussian in the spectrum of $\phi = 0°$ in Figure 3 at approximately 8.75 eV is not supported by the other spectrum in the same figure neither by the PES and theoretical calculations, and the discrepancy did not appear beyond three standard deviation bars. As a result, we believe it is mainly due to the statistical fluctuation and do not consider it as a peak in the present study.

The uniqueness of the assignment to peak 1 is also evidenced by intensities. The ratio between the intensities (counts) of peak 1 and the most intensive peak 4 in Figure 3b is approximately 1:6, which remains almost the same in Figure 3a. The consistency in the spectral ratio at $\phi = 0°$ and at $\phi \neq 0°$ indicates that the symmetry of this orbital is dominated by a totally symmetric orbital, such as a for C_2 and a′ for the C_s conformer, otherwise the ratio cannot remain if the peak is (i) an orbital with a b symmetry for C_2 and an a″ for the C_s conformer and (ii) a cluster of unresolved orbitals containing orbitals with b or a″ symmetry. In addition, in a most recent EMS measurement for bicyclo[2.2.1]hepta-2,5-dione from one of the world's leading EMS groups,[34] the overlaps between the binding energy spectra at either $\phi = 0°$ and $\phi \neq 0°$ in the band of 11−15 eV of bicyclo[2.2.1]hepta-2,5-dione are more significant than the present study. However, the unique assignment of the EMS binding energy spectra (Figure 4 in ref 34) was achieved with the help of higher resolution PES spectra as well as quantum mechanical calculations.

Figure 4 displays the EMS experiment orbital cross-sections of the HOMO as a function of momentum **p**, together with the simulated orbital MDs of the HOMOs of the C_2 and C_s conformers, respectively, under the experimental conditions (room temperature, $T = 298$ K). It is not unfamiliar from our previous experience[30−35,52,54] that the s^xp^y hybridized orbital

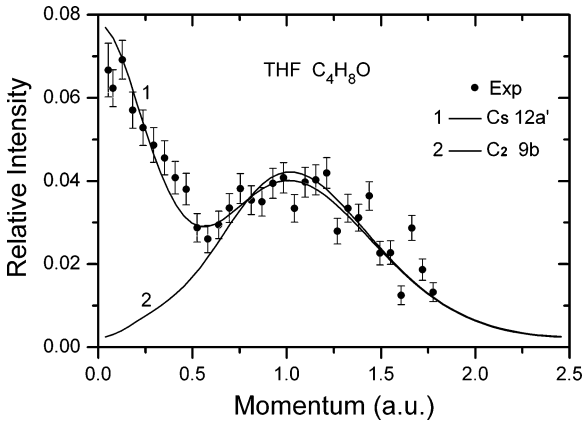

Figure 4. Experimental and simulated orbital momentum distributions for the highest occupied molecular orbitals (HOMO) of tetrahydrofuran C_s and C_2 conformers. The theoretical orbital momentum distributions for C_s (curve 1) and C_2 (curve 2) are simulated using the B3LYP/6-311++G**//MP2/aug-cc-pVTZ model.

behavior of the experimental cross-sections well fit into the simulated HOMO (12a′) orbital MDs of the C_s conformer. The HOMO (9b) orbital MDs of the C_2 conformer exhibit a typical bell-shaped p-like orbital nature, which does not agree with the measurements. As a result, the orbital MDs in Figure 4 lead to the conclusion that the most populated conformer of tetrahydrofuran in the gas phase is dominated by the C_s conformer. The binding energy spectra of THF in the outer valence space given by Table 2 are, therefore, assigned to the orbitals of the C_s conformer in the column highlighted. Combining theoretical models with two different experiments, we are able to assign the ionization spectra of tetrahydrofuran for the first time, two decades after the PES measurements[42] were published. The results are given in Table 2.

The differences in the HOMO orbital MDs between the C_s and C_2 conformers imply that the chemical bonding mechanisms underlining the conformers are not the same. Figure 5 further explores the orbital electron density contours in the more familiar coordinate space. The orbital electron density distributions of the HOMOs, 12a′, 9b, of conformer C_s and C_2 indeed look very similar with dominated contributions from the C(2)-H_2−O(1)−C(3)H_2 network in both HOMOs: the two 1s H orbital enhanced p_z orbitals of C(2) and C(3) in the CH_2 groups connected the O(1) p_z lone pair. However, the participation of the p_y orbitals of C(4) and C(5) in the HOMO of 12a′ of

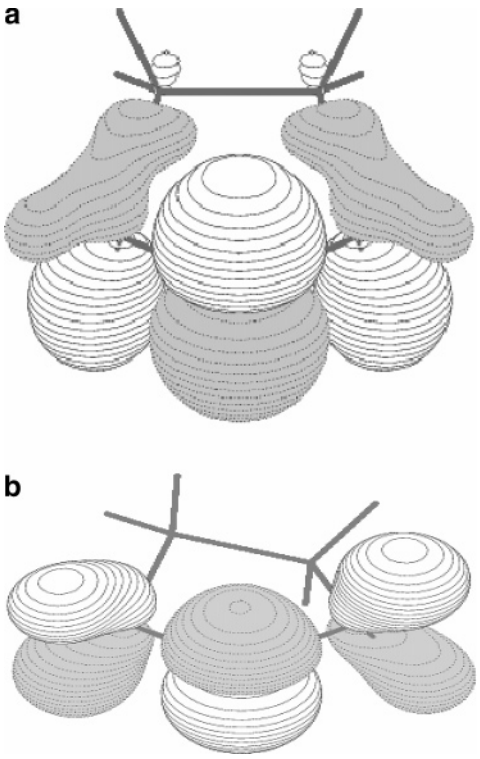

Figure 5. Orbital electron charge distributions of the highest occupied molecular orbitals (HOMO) of tetrahydrofuran (a) C_s conformer and (b) C_2 conformer. The orbital electron densities are produced using the B3LYP/6-311++G**//MP2/aug-cc-pVTZ model. Molden[57] is used to plot the contours.

conformer C_s, which is only possible in the C_s structural arrangement, forming a "pseudo" σ bond with the p_z orbitals of C(2) and C(3), respectively, further distorts the antibonding nature of the enhanced p-like distribution (Figure 5a). The orbital MDs in Figure 4 reflect this distortion with a local minimum. The C_2 conformer does not permit orbitals of C(4) and C(5) to overlap sufficiently with the $C(2)H_2-O(1)-C(3)H_2$ network in HOMO (9b) as shown in Figure 5b, leaving this orbital (9b) with little distortion.

Orbital momentum distributions of the complete valence space will be able to provide a more comprehensive picture for the conformers and possibly dynamics of THF. However, the possibility of interchanging or coexistence (due to low-energy barriers on the conformational potential energy cross-section[9]) of the conformers, combined with the unresolved and clustered orbitals (due to the congested binding energy spectra of THF), raises the questions to the uniqueness of the experimental momentum distributions of other valence orbitals apart from the HOMO. Theoretically, the configuration of the simulated orbitals from the available conformers of THF is also not unique. In addition, the impact energy of 600 eV in the present measurement may not be sufficiently high when entering into a higher energy band in the valence space. A theoretical study to explore the orbital behavior of the THF conformers in the valence space is under investigation at the moment. Without further experimental results to improve the uniqueness of the orbital momentum distributions, any comparison made at this point would not be practically meaningful.

5. Conclusions

The most populated conformer of tetrahydrofuran generated from pseudorotation has been identified as the C_s conformer in the gas phase, diagnosed by the present joint electron momentum spectroscopy and theoretical calculations. Quantum mechanical calculations, including density functional theory based on B3LYP and SAOP and outer valence Green function (OVGF) methods, play a significant role in the identification of the most stable structure and hereby the assignment of the ionization spectra in the outer valence space of tetrahydrofuran.

The C_s conformer has been singled out from three possible conformations of tetrahydrofuran, that is, the C_1, C_2, and C_s structures which are competitive in energy. In coordinate space, the energy differences among the conformations are very small and possibly interchangeable, which leads to all possibilities for the C_1,[8,14] C_2,[1,12,15] and C_s[9] structures to be reported as the most stable structure for tetrahydrofuran. Experiments such as microwave and far-infrared spectroscopy[8,12,14−15] and photoelectron spectroscopy (PES)[42] have been unable to identify the most stable structure of tetrahydrofuran without contradictions.[9] Theoretical results of tetrahydrofuran,[1,9,55] which have also predicted almost all possibilities, may be insufficient to make solid conclusions without experimental support.

Dual space analysis (DSA) has demonstrated the importance of accessing complementary information from coordinate and momentum space. The present theoretical optimizations using the B3LYP/6-311++G** model exclude the C_1 conformation from the group of three conformations due to its imaginary lowest frequency, indicating a transition state, in agreement with Rayon and Sordo.[9] The fact that the C_2 and C_s conformers exhibit similarities in their energies and other molecular properties including dipole moments implies that such molecular properties fail to differentiate the target conformers. However, the most obvious difference between C_2 and C_s conformers of tetrahydrofuran is indeed their symmetry and electron distributions. The molecular electron charge (derived) potentials (MEP) of the two species are very different, and therefore, the symmetry of the highest occupied molecular orbitals of C_2 (9b) and C_s (12a′) species is identified to carry the fingerprint of the conformers. Assisted by the OVGF/6-31G* and SAOP/ET-PVQZ model predicted ionization energies in the outer valence space, the HOMOs of the C_2 and C_s conformers happen to be the only EMS experimentally resolved orbital for tetrahydrofuran in the valence space. The EMS measurement identifies the fingerprint of the C_s conformer to be the most populated conformer in the gas phase from the simulated HOMO MDs of the C_s and C_2 conformers. This discovery leads to the orbital-based assignment to the PES and EMS experimental binding energy spectra, based on our OVGF/6-31G* and SAOP/ET-PVQZ models. The present study demonstrates the complementary nature of experiment and theory, information in coordinate space and momentum space. This study also explores an innovative approach to study molecular stabilities of biological systems which are rich in conformers.

Acknowledgment. F.W. acknowledges the Australian Research Council (ARC) for an International Linkage Award and the Australian Partnership for Advanced Computing (APAC) for use of the (Australian) National Supercomputing Facilities. F.W. thanks Professor Jose A. Sordo for providing their group's ab initio results of the conformers. Project 10575062 is supported by the National Natural Science Foundation of China, and Project 20050003084 is supported by the Specialized Research Fund for the Doctoral Program of Higher Education.

References and Notes

(1) Cadioli, B.; Gallinella, E.; Coulombeau, C.; Jobic, H.; Berthier, G. *J. Phys. Chem.* **1993**, *97*, 7844.

(2) Mozejko, P.; Sanche, L. *Radiat. Phys. Chem.* **2005**, *73*, 77.

(3) Bouchiha, D.; Gorfinkiel, J. D.; Caron, L. G.; Sanche, L. *J. Phys. B: At. Mol. Opt. Phys.* **2006**, *39*, 975.

(4) Jawetz, E. Antiviral chemotherapy and prophylaxis. *Basic and Clinical Pharmachology*; Katzung, B. G., Ed.; Appleton & Lange: Englewood Cliffs, NJ, 1992; p 674.

(5) Lafferty, W. J.; Robinnson, D. W.; St. Louis, R. V.; Russel, J. W.; Strauss, H. L. *J. Chem. Phys.* **1965**, *42*, 2915.

(6) Diez, E.; Esteban, A. L.; Bermejo, F. J.; Rico, M. *J. Phys. Chem.* **1980**, *84*, 3191.

(7) Seong, J. H.; Young, K. K. *THEOCHEM* **1996**, *369*, 157.

(8) Meyer, R.; Lopez, J. C.; Alonso, J. L.; Melandri, S.; Favero, P. G.; Garminati, W. *J. Chem. Phys.* **1999**, *111*, 7871.

(9) Rayón, V. M.; Sordo, J. A. *J. Chem. Phys.* **2005**, *122*, 204303.

(10) Zecca, A.; Perazzolli, C.; Brunger, M. J. *J. Phys. B: At., Mol. Opt. Phys.* **2005**, *38*, 2079.

(11) Tranter, G. E.; Macdermott, A. J. *Chem. Phys. Lett.* **1986**, *130*, 120.

(12) Melnik, D. G.; Gopalakrishnan, S.; Miller, T. A.; De Lucia, F. C. *J. Chem. Phys.* **2003**, *118*, *3589.*

(13) Wu, A.; Cremer, D. *Int. J. Mol. Sci.* **2003**, *4*, 158.

(14) Engerholm, G. G.; Luntz, A. C.; Gwinn, W. D.; Harris, D. O. *J. Chem. Phys.* **1969**, *50*, 2446.

(15) Mamleev, A. H.; Gunderova, L. N.; Galeev, R. V. *J. Struct. Chem.* **2001**, *42*, 365.

(16) Luger, P.; Buschmanm, J. *Angew. Chem., Int. Ed. Engl.* **1983**, *22*, 410.

(17) Wang, F. *J. Phys. Chem. A* **2003**, *107*, 10199.

(18) Wiberg, K. B.; Rablen, P. R. *J. Comput. Chem.* **1993**, *14*, 1505.

(19) Falzon, C. T.; Wang, F. *J. Chem. Phys.* **2005**, *123*, 214307.

(20) Klein, R. A.; Zottola, M. A. *Chem. Phys. Lett.* **2006**, *419*, 254.

(21) Coulson, C. L. *Rev. Mod. Phys.* **1960**, *32*, 170.

(22) Ren, X. G.; Ning, C. G.; Deng, J. K.; Zhang, S. F.; Su, G. L.; Huang, F.; Li., G. Q. *Rev. Sci. Instrum.* **2005**, *76*, 063103.

(23) Ning, C. G.; Deng, J. K.; Su, G. L.; Zhou, H.; Ren, X. G. *Rev. Sci. Instrum.* **2004**, *75*, 3062.

(24) Deng, J. K.; Li, G. Q.; He, Y.; Huang, J. D.; Deng, H.; Wang, X. D.; Wang, F.; Zhang, Y. A.; Ning, C. G.; Gao, N. F.; Wang, Y.; Chen, X. J.; Zheng, Y. *J. Chem. Phys.* **2001**, *114*, 882.

(25) Bevington, P. R.; Robinson, D. K. *Data Reduction and Error Analysis for the Physical Sciences*; McGraw-Hill: New York, 1990.

(26) Ren, X. G.; Ning, C. G.; Deng, J. K.; Zhang, S. F.; Su, G. L.; Huang, F.; Li, G. Q. *Phys. Rev. Lett.* **2005**, *94*, 163201.

(27) Ning, C. G.; Ren, X. G.; Deng, J. K.; Zhang, S. F.; Su, G. L.; Huang, F.; Li, G. Q.; *Chem. Phys. Lett.* **2005**, *407*, 423.

(28) Ning, C. G.; Ren, X. G.; Deng, J. K.; Su, G. L.; Zhang, S. F.; Li, G. Q. *Phys. Rev. A* **2006**, *73*, 022704.

(29) Ning, C. G.; Ren, X. G.; Deng, J. K.; Zhang, S. F.; Su, G. L.; Huang, F.; Li, G. Q. *J. Chem. Phys.* **2005**, *122*, 224302.

(30) Sagar, R. P.; Guevara, N. L. *ArXiv Quantum Physics e-prints*; 2006, quant-ph/0602046.

(31) Falzon, C. T.; Wang, F.; Pang, W. N. *J. Phys. Chem. B* **2006**, *110*, 9713.

(32) Falzon, C. T.; Wang, F. *J. Chem. Phys.* **2005**, *123*, 214307.

(33) Jones, D. B.; Wang, F.; Brunger, M. J.; Winkler, D. A. *Biophys. Chem.* **2006**, *121*, 105.

(34) Jones, D. B.; Bolorizadeh, M. A.; Brunger, M. J.; Saha, S.; Wang, F.; Gleiter, R.; Bueber, J.; Winkler, D. A. *J. Phys B: At., Mol. Opt. Phys.* **2006**, *39*, 2411.

(35) Saha, S.; Wang, F.; Falzon, C.; Brunger, M. J. *J. Chem. Phys.* **2006**, *123*, 124315.

(36) de la Vega, J. M. G.; Miguel, B. *Eur. J. Phys.* **1998**, *19*, 395.

(37) Cederbaum, L. S.; Domcke, W. *Advances in Chemical Physics*; John Wiley and Sons: New York, 1977.

(38) von Niessen, W.; Schirmer, J.; Cederbaum, L. S. *Comput. Phys. Rep.* **1984**, *1*, 57.

(39) Gritsenko, O. V.; van Leeuwen, R.; Baerends, E. J. *J. Chem. Phys.* **1994**, *101*, 8955.

(40) Gritsenko, O. V.; van Leeuwan, R.; Baerends, E. J. *Phys. Rev. A* **1995**, *52*, 1870.

(41) Baerends, E. J.; Autschbach, J.; Brces, A.; Bo, C.; Boerrigter, P. M.; Cavallo, L.; Chong, D. P. *ADF2004.01*, Version 03, SCM: Vije Universiteit: Amsterdam, The Netherlands, 2003.

(42) Kimura, K.; Katsuwata, S.; Achiba, Y.; Yamazaki, T.; Iwata, S. *Handbook of HeI Photoelectron Spectra of Fundamental Organic Molecules*; Halsted Press: New York, 1981.

(43) Frisch, M. J.; Trucks, G. W.; Schlegel, H. B.; Scuseria, G. E.; Robb, M. A.; Cheeseman, J. R.; Montgomery, J. A., Jr.; Vreven, T.; Kudin, K. N.; Burant, J. C.; Millam, J. M.; Iyengar, S. S.; Tomasi, J.; Barone, V.; Mennucci, B.; Cossi, M.; Scalmani, G.; Rega, N.; Petersson, G. A.; Nakatsuji, H.; Hada, M.; Ehara, M.; Toyota, K.; Fukuda, R.; Hasegawa, J.; Ishida, M.; Nakajima, T.; Honda, Y.; Kitao, O.; Nakai, H.; Klene, M.; Li, X.; Knox, J. E.; Hratchian, H. P.; Cross, J. B.; Adamo, C.; Jaramillo, J.; Gomperts, R.; Stratmann, R. E.; Yazyev, O.; Austin, A. J.; Cammi, R.; Pomelli, C.; Ochterski, J. W.; Ayala, P. Y.; Morokuma, K.; Voth, G. A.; Salvador, P.; Dannenberg, J. J.; Zakrzewski, V. G.; Dapprich, A.; Daniels, A. D.; Strain, M. C.; Farkas, O.; Malick, D. K.; Rabuck, A. D.; Raghavachari, K.; Foresman, J. B.; Ortiz, J. V.; Cui, Q.; Baboul, A. G.; Clifford, S.; Cioslowski, J.; Stefanov, B. B.; Liu, G.; Liashenko, A.; Piskorz, P.; Komaromi, I.; Martin, R. L.; Fox, D. J.; Keith, T.; Al-Laham, M. A.; Peng, C. Y.; Nanayakkara, A.; Challacombe, M.; Gill, P. M. W.; Johnson, B.; Chen, W.; Wong, M. W.; Gonzalez, C.; Pople, J. A. *Gaussian 03*, Revision C.02; Gaussian: Wallingford, CT, 2004.

(44) McCarthy, I. E.; Weigold, E. *Rep. Prog. Phys.* **1991**, *54*, 789.

(45) Weigold, E.; McCarthy I. E. *Electron Momentum Spectroscopy*; Kluwer Academic−Plenum: New York, 1999.

(46) Dolgounitcheva, O.; Zakreski, V. G.; Ortiz, J. V. *J. Am. Chem. Soc.* **2000**, *122*, 12304.

(47) Bawagan, A. O.; Brion, C. E.; Davidson, E. R.; Feller, D. *Chem. Phys.* **1987**, *113*, 19.

(48) Ning, C. G.; Ren, X. G.; Deng, J. K.; Su, G. L.; Zhang, S. F.; Knippenberg, S.; Deleuze, M. S. *Chem. Phys. Lett.* **2006**, *421*, 52.

(49) Duffy, P.; Chong, D. P.; Casida, M. E.; Salahub, D. R. *Phys. Rev. A* **1994**, *50*, 4707.

(50) Brion, C. E. *Int. J. Quantum Chem.* **1986**, *29*, 1397.

(51) MiGdall, J. N.; Coplan, M. A.; Hench, D. S. *Chem. Phys.* **1981**, *57*, 141.

(52) Ngugen, T. V.; Pratt, D. W. *J. Chem. Phys.* **2006**, *124*, 054317.

(53) Chong, D. P. *J. Electron Spectrosc. Relat. Phenom.* **2005**, *146*, 115.

(54) Wang, F.; Brunger, M. J.; McCarthy, I. E.; Winkler, D. A. *Chem. Phys. Lett.* **2003**, *382*, 217.

(55) Han, S. J.; Kang, Y. K. *J. Mol. Struct. (THEOCHEM)* **1996**, *369*, 157.

(56) Wang, F.; Downton, M.; Kidwani, N. *J. Theor. Comput. Chem.* **2005**, *4*, 247.

(57) Schaftenaar, G.; Noordik, J. *J. Comput.-Aided Mol. Des.* **2000**, *14*, 123.

(58) Zheng, Y.; Neville, J. J.; Brion, C. E. *Science* **1995**, *270*, 786.